LBL--14512

LBL-14512

DE82 018521

Formation of a Quark-Gluon Plasma in Nuclear Collisions

M. Gyulassy

Nuclear Science Division
Lawrence Berkeley Laboratory
University of California
Berkeley, CA 94720

This work was supported by the Director, Office of Energy Research, Division of Nuclear Physics of the Office of High Energy and Nuclear Physics of the U.S. Department of Energy under Contract DE-AC03-76SF00098.

LBL-14517

FORMATION OF A QUARK-GLUON PLASMA IN NUCLEAR COLLISIONS

M. Gyulassy
Nuclear Science Division, Lawrence Berkeley Laboratory
University of California, Berkeley, CA 94720

ABSTRACT

The spacial dependence of the energy deposition in the fragmentation regions is estimated for nuclear collisions at ISR energies, $\sqrt{s}/A \gtrsim 30$ GeV/nucleon. Two models (the trailing cascade and sequential decay scenarios) are contrasted. The results are compared to the quark-gluon plasma energy density computed via QCD lattice methods.

There are three major questions that need to be discussed in connection with the formation of a quark-gluon plasma via nuclear collisions. First, how efficient are nuclear collisions in generating high energy densities? Second, what is the critical QCD energy density at which hadronic matter dissolves into a quark-gluon plasma? Finally, which observables could tell us that a plasma was indeed formed? In the past two years, considerable progress has been made toward answering these questions, but much work still remains to be done. This lecture is intended to provide an introduction to some basic concepts and theoretical considerations that are currently under debate.

The most basic concept needed in discussions of nuclear collisions at energies $E_{Lab} \gtrsim 100$ GeV per nucleon is the growth of longitudinal distances.[1] From this concept follows the transparency of nuclei and the limited cascading of secondaries. With regard to q-g plasma formation the most important consequence is the limitation on the energy density that can be achieved. This limitation was first recognized in the work of McLerran, et al.[2] that was based on the parton model of hadronic processes.

Longitudinal growth can be understood as follows: In an inelastic reaction between two hadrons, one with rapidity $y_T = \tanh^{-1} v_T = 0$ and the other with rapidity $y_p \gg 1$, partons with rapidity between y_T and y_p are produced with a distribution dN/dy. These partons begin to separate and after some time, $\tau(y)$, a group of partons in a rapidity interval $\Delta y \sim 1/2$ coalesce to form a hadron (pion) with velocity $v = \text{th } y$. To estimate $\tau(y)$, we assume that in the rest frame of the produced hadron it takes a characteristic time, $\tau_0 \sim 1$ fm/c, for the partons to arrange themselves according to the wavefunction of that hadron. Viewed in the frame where that hadron has rapidity y and perpendicular momentum $p_\perp$, this time is dilated according to

$$\tau(y) = \frac{\varepsilon(y)}{m}\,\tau_0 \cong \frac{m_\perp}{m}\,\frac{e^y}{2}\,\tau_0 \quad , \tag{1}$$

where $m_\perp^2 = m^2 + p_\perp^2$ (recall $\varepsilon = m_\perp \text{ ch } y$, $p_\parallel = m_\perp \text{ sh } y$). Since the velocity $v_\parallel(y) \cong 1 - 2e^{-2y}$ is close to the speed of light, c = 1, the formation distance of secondaries, $d_\parallel(y) = \tau(y) \text{ th } y$, along beam direction, grows very rapidly with y. Therefore, a secondary can "materialize" in a target nucleus of thickness $2R \approx 2.4\ A^{1/3}$ fm only if $d_\parallel(y) < 2R$ or

$$y < \ell n \frac{4R}{\tau_0} \equiv y_c \quad , \tag{2}$$

For Uranium, $y_c \approx 3.4$. Of course, a secondary produced within the nucleus at depth z into the target only has a distance $2R - z$ to materialize, and hence $y_c^*(z) = y_c^* + \ell n\,(1 - z/2R)$ is smaller than for a secondary produced at x = 0.

On the other hand, a parton packet does not have to be in its ground state before interactions with target nucleons can occur. The transit time of the packet through the nucleus is $t(y) = 2R/\text{th } y$. During this time the packet is displaced relative to the projectile by an amount

$$\Delta r_\parallel(y) = [v_p - v_\parallel(y)]\,t(y) \cong 4R\,e^{-2y} \tag{3}$$

$$\Delta r_\perp(y,p_\perp) = \frac{p_\perp}{\varepsilon(y,p_\perp)}\,t(y) = \frac{p_\perp}{m_\perp}\,4R\,e^{-y} \quad . \tag{4}$$

Thus, $\Delta r_{\parallel} \sim e^{-y} \Delta r_{\perp}$, and the transverse separation is much greater than the longitudinal one. This point was emphasized by McLerran et al.[2] Note that for partons that are slow enough (eq. (2)) to *materialize in the target* $\Delta r_{\parallel} \sim \tau_0^2/2R << 1$ fm, while $\Delta r_{\perp} \gtrsim \tau_0 \sim 1$ fm. Therefore, if we assume that secondary interactions occur as soon as $\Delta r_{\perp} > \tau_0 \sim 1$ fm, then

$$y < \ell n \frac{4R}{\tau_0} \frac{p_{\perp}}{m_{\perp}} \approx y_c \quad . \tag{5}$$

Therefore, the materialization condition in the target, eq. (2), is equivalent to the requirement that the centers of the projectile and secondary packets separate by $\Delta r_{\perp} \sim 1$ fm in the transverse direction.

For hadron-nucleus collisions, this requirement clearly insures secondary cascading since the incident hadron has limited perpendicular extent, $\sim\tau_0$. Therefore, when a secondary hadron is displaced by τ_0 in the perpendicular direction, a new row of target nucleons will start participating in the reaction. However, for a nucleus-nucleus collision, the significance of such a transverse displacement is less clear. The incident projectile nucleus is a Lorentz contracted pancake with a large transverse extension $R >> \tau_0$. The thickness of that pancake is limited to ~1 fm since the projectile wavefunction in the target frame contains many slow "wee" partons (near Feynman $x_F \sim 0$). Therefore, it takes each target nucleon on the order of $\tau_0 \sim 1$ fm/c to interact with the projectile nucleus. Now consider a parton packet of mean rapidity y_c produced immediately after the projectile nucleus enters the target (at depth $z = 0$). By the time ($\sim 2R$) the projectile exits the target and the center of that packet is displaced $\Delta r_{\parallel}$ and $\Delta r_{\perp}$ relative to the projectile. However, in this case, because the projectile has a large perpendicular extent $R >> \tau_0$, the parton cloud is still immersed in the projectile pancake as far as a target nucleon is concerned. Therefore, a target nucleon on the exit side may not respond incoherently to that parton packet. Simply put, the target nucleon will not have had enough time to complete its response to the projectile before that secondary hits it. In this situation a detailed dynamical theory is needed to determine the actual response of the target nucleons. On

the other hand, there is still a nontrivial kinematic domain where incoherent interactions (i.e. cascading) can be expected. If the parton packet lags <u>behind</u> the projectile by $\Delta r_{\parallel} \sim 1$ fm, then a target nucleon will respond incoherently to the projectile and to the trailing packet. This is because the characteristic response time of a hadron is also on the order of the parton rearrangement time τ_0 discussed before. The condition for lagging behind the projectile is $\Delta r_{\parallel}(y) > \tau_0$, which with eq. (3) is

$$y < \frac{1}{2} \ln \frac{4R}{\tau_0} = \frac{1}{2} y_C \quad . \tag{5}$$

Note the factor of 1/2 that arose from the Lorentz kinematic difference between longitudinal and transverse displacements, eqs. (3,4). Incoherent scattering could also result if $\Delta r_{\perp}(y) > R_{proj} \gg \tau_0$, but for large nuclei, this is even more restrictive than eq. (5).

Up to this point, we have assumed that the target remains at rest after the interaction. We must of course include recoil effects. An inelastic collision converts on the average a fraction, η, of the incident kinetic energy into hadrons. This inelasticity reduces the kinetic energy per nucleon in the center of mass sytem by exp $(-\Delta y_r)$, where Δy_r is the recoil rapidity shift. Energy conservation relates Δy_r to η via $\sqrt{s}\ (2e^{-\Delta y} + \eta) = \sqrt{s}$, giving

$$\Delta y_r = \ln \frac{1}{1-\eta} \quad . \tag{7}$$

At ISR energies, $\Delta y_r < 1$.

As the projectile sweeps through the target, each hit target nucleon acquires a rapidity Δy_r. For a parton packet with a mean rapidity y produced at z = 0, it takes at least a time t = 2R/th y to reach a target nucleon on the opposite side of the nucleus at z = 2R. The exact time is determined by the catch-up condition

$$v\,t = 2R + v_r\,(t - 2R/v_p) \quad , \tag{8}$$

where $2R/v_p$ is the time at which the projectile interacts with the last target nucleon and v_r = th Δy_r. Therefore, in the lab frame,

$$\Delta t = t - 2R/v_p = \frac{2R}{v_p} \frac{v_p - v}{v - v_r} \tag{9}$$

is the time lag between interactions of the last target nucleon with the projectile and with the secondary parton packet of rapidity y. In the target recoil rest frame, a shorter time lag, $\Delta t/\gamma_r$, is experienced between these interactions. If $\Delta t/\gamma_r < \tau_0$, then the target responds most likely coherently to these interactions. On the other hand, if $\Delta t/\gamma_r > \tau_0$, then the recoil target nucleon will respond most likely incoherently to these interactions. Therefore, the conservative cascading condition including recoil is $\Delta t/\gamma_r > \tau_0$ with Δt given by eq. (9). This condition restricts cascading rapidities to

$$y < \frac{1}{2}(y_c + \Delta y_r) = \frac{1}{2}\ln\frac{4R}{\tau_0} + \frac{1}{2}\ln\frac{1}{1-\eta} \equiv y_c^r \quad , \tag{10}$$

where we used $\gamma_r(1 - v_r) = 1 - \eta$ from eq. (7). For U + U, $y_c^r = 2.0 \pm 0.5$: for $\eta = 2/3$, $\tau_0 = 0.5$–2.0 fm.

We now turn to a more detailed dynamical formulation of energy deposition in the fragmentation regions. The problem is to determine how much energy and momentum are deposited in the target as a function of the depth into it. Suppose that a target nucleon at depth z_i suffers a collision with the projectile. The time of that collision is $t_i = z_i/v_p$. The projectile transfers a recoil energy and momentum to that nucleon such that the energy momentum per nucleon becomes

$$E_r/A = \gamma_r m_N \quad , \quad P_r/A = \gamma_r v_r m_N \quad , \tag{11}$$

If no secondaries interact in the target, then this recoil alone results in a lab compression of the target by a factor $(1 - v_r/v_p)^{-1}$. This is because the target nucleon at depth $z = 2R$ begins to recoil only at time $2R/v_p$, and by that time the target nucleon initially at depth $z = 0$ has moved to $z = v_r(2R/v_p)$, reducing the nuclear size to $(1-v_p/v_p)2R$.

To incorporate interactions with secondaries, note first that secondaries, produced at z_i with a distribution dN/dy, follow the projectile along the trajectory

$$z_i(t) = (t - t_i)\ \text{th}\ y + z_i \tag{12}$$

for $t > t_i$. The <u>dynamical</u> assumption we now make is that the time t(y) when the secondary interacts in the target and transfers all

its energy-momentum is a monotonic increasing function of y. The conservative cascade criteria discussed in connection with eq. (5) lead to

$$t(y) - t_i = \frac{\Delta_r}{v_p - \text{th } y} \approx \frac{1}{2} e^{2y} \Delta_r \quad , \tag{13}$$

where $\Delta_r = \tau_0/\gamma_r$ is the distance by which a secondary must trail behind the projectile in order to cascade incoherently in the rest frame of the recoiled target. Equation (13) defines the Trailing Cascade Model (TCM).

An optimistic cascade criterion that could be postulated is that as soon as a secondary has had enough time, τ_0, in its own rest frame to rearrange its parton wavefunction (i.e. decay) it will be stopped in the recoiling target. This criterion simply generalizes eq. (1) to

$$t(y) - t_i = \Delta_\perp \text{ ch } y \quad , \tag{14}$$

with $\Delta_\perp = \tau_0 m_\perp/m$. Equation (14) defines the Sequential Decay Model (SDM) and corresponds to the scenario developed in Ref. (2).

In either case, replacing t in eq. (12) by t(y) gives the depth $z_i(y)$ at which a secondary of rapidity y, which was produced at z_i, deposits its energy-momentum in the target. Since we are given the rapidity density dN/dy of secondaries, the number of secondaries decaying per unit depth is simply

$$\frac{dN}{dz}(z - z_i) = \frac{dN}{dy}[y(z - z_i)] \frac{dy(z-z_i)}{dz} \theta(z - z_i) \tag{15}$$

For the conservative TCM, eq. (12,13) give for $t_i = z_i = 0$

$$z(y) = v_p t(y) - \Delta_r \quad , \tag{16a}$$

$$y(z) = \frac{1}{2} \ln \frac{t+z}{t-z} \approx \frac{1}{2} \ln (1+2z/\Delta_r \quad , \tag{16b}$$

$$\frac{dy}{dz} = \frac{v_p \Delta_r}{t^2(y) - z^2(y)} \approx \frac{1}{2z(y)+\Delta_r} \quad , \tag{16c}$$

For the optimistic SDM scenario,

$$z(y) = \sqrt{t^2(y) - \Delta_\perp^2} \quad , \tag{17a}$$

$$y(z) = \ell n \left(\sqrt{1 + (z/\Delta_\perp)^2} + z/\Delta_\perp \right) , \tag{17b}$$

$$\frac{dy}{dz} = (z^2 + \Delta_\perp^2)^{-1/2} \quad . \tag{17c}$$

Note that in both models dy/dz and hence dN/dz falls off as ~1/z from the interaction point. Thus, fewer secondaries interact in the target at greater depths. However, the energy-momentum carried by each secondary increases with depth because $\epsilon(y) \approx p(y) \sim e^{y(z)}$. The energy-momentum deposition is in fact

$$\begin{bmatrix} \frac{dE}{dz} \\ \\ \frac{dP}{dz} \end{bmatrix} = \sum_i m_\perp \begin{bmatrix} \mathrm{ch}\Gamma y(z-z_i)\Gamma \\ \\ \mathrm{sh}\Gamma y(z-z_i)\Gamma \end{bmatrix} \frac{dN}{dz}(z - z_i) \quad , \tag{18}$$

where the sum is over all struck target nucleons. If the target nucleons are distributed uniformly between $0 < z_i < 2R$ with ρ_0 $\mathcal{A}$ particles per unit length ($\rho_0 = 0.145\ fm^{-3}$, $\mathcal{A} = 2/3\pi R^2$, $R = 1.18\ A^{1/3}$ fm), then the sum can be converted into an integral. Dividing by the area, changing $z \to z'$ the energy deposition per unit <u>volume</u> due to secondary cascading is

$$\frac{E}{V}(z) = \frac{1}{\mathcal{A}} \frac{dE}{dz}(z) = \rho_0 \int_0^{y(z)} \langle m_\perp \rangle \, \mathrm{ch}\, y \, \frac{dN}{dy} \, dy \quad . \tag{19}$$

Dividing by ρ_0 gives the energy per baryon E/A deposited at z. Also replacing ch by sh in eq. (9) gives the momentum density P/V(z). Note that this is a lab frame quantity. The specific dynamical model enters through y(z).

We must now specify dN/dy. This should be taken from pp data at the relevant cm energy. However, we consider here for illustration only a schematic model represented by a uniform rapidity density

$$m_\perp \frac{dN}{dy} \approx 2m_\pi \frac{\langle n_\pi \rangle}{2y^*} \tag{20}$$

with $\langle n_\pi \rangle \approx 12\ (\sqrt{s}/30\ \mathrm{GeV})^{1/2}$ and $y^* = \ell n\, \sqrt{s}/m_N$. For

$\sqrt{s}$ = 30 GeV/nucleon, $m_\perp$ dN/dy ~ 0.5 GeV. Detailed calculations based on pp data will be reported elsewhere. With eq. (20), the inelasticity η needed in eq. (7) is given simply by

$$\eta = \frac{m_\pi \langle n_\pi \rangle}{m_N\, y^*} \quad . \tag{21}$$

For $\sqrt{s}$ = 30,60 GeV, η = 0.53,0.62. Comparing eqs. (20,21), we see that m dN/dy = ηm_N for this model. The integral in eq. (19) is then elementary giving

$$E/A(z) = \eta m_N \text{ sh } y(z) = \frac{\eta m_N z}{\sqrt{t(z)^2 - z^2}} \quad ,$$

$$P/Z(z) = \eta m_N \text{ (ch } y(z) - 1) = \eta m_N \left(\frac{t(z)}{\sqrt{t(z)^2 - z^2}} - 1 \right) \quad , \tag{22}$$

where t(z) is given by eqs. (16a,17a) for the TCM, SDM, respectively. For depths $z >> \Delta_r, \Delta$ ~ 1 fm, $E/A(z) \approx P/A(z) \propto \sqrt{z/\Delta_r}$ and $z/\Delta_\perp$ for these two models.

The mean flow velocity of the target slab at depth z after absorbing both recoil and cascading energy-momentum is thus given by

$$v_f(z) = \text{th } y_f(z) = \frac{\text{sh } \Delta y_r + \eta(\text{ch } y(z) - 1)}{\text{ch } \Delta y_r + \eta \text{ sh } y(z)} \quad , \tag{23}$$

where Δy_r is related to η via eq. (7). The invariant mass per nucleon of the slab initially at depth z is

$$M^*(z) = \left[(E_r/A + E/A(z))^2 - (P_r/A + P/A(z))^2 \right]^{1/2} \quad . \tag{24}$$

The compression achieved at a given depth is clearly maximum at the time when the energy-momentum due to recoil and cascading is absorbed by the target matter at that depth. If we compare two slabs separated by Δz, then as with recoil alone a compression $\rho/\rho_0 = (1 - v_f(z)/v_p)^{-1}$ is achieved in the lab. Therefore, in the comoving frame, in which $v_f(z) = 0$, the maximum compression achieved is

$$\rho^*(z) = \rho_0(\gamma_f(z)(1 - v_f(z)/v_p))^{-1} \quad , \tag{25}$$

where $\gamma_f^{-1} = (1 - v_f^2)^{1/2}$. Therefore, the maximum energy density

achieved in the comoving frame is

$$E^*/V(z) = \rho^*(z)\, M^*(z) \quad . \tag{26}$$

The results are shown in Figure 1. The solid curves refer to $\sqrt{s}$ = 30 GeV per nucleon. The dashed curves refer to $\sqrt{s}$ = 100 GeV per nucleon. The *Trailing Cascade model* results are given by curves 1 and 2. The Sequential Decay model results are given by curves 3 and 4. In part (a) the maximum energy density $E^*/V(z)$ in the local comoving frame is given. The depth z is only the initial location of the slab. At a later time each slab element moves with a different mean flow velocity as shown in 1c. Note that for TCM an approximate uniform energy density, compression (part b), and flow rapidity (part c) is found. However, $E^*/V \lesssim 1$ GeV/fm^3 is rather small for this ISR energy range even up to $U^{238} + U^{238}$ collisions. On the other hand, the optimistic SDM scenario leads to more than a factor of two higher energy densities, $E/V \lesssim 3$ GeV/fm^3. At the same time, though, significant spacial gradients are generated. The monotonic increase of $y_f(z)$ indicates for example that in the local comoving frame of any given slab element all other slabs are receding! Note, by the way, that very little is gained by increasing the mass of the colliding nuclei from Xe^{131} to U^{238}. Even a super-duper-heavy (Gr^{609}) would not yield much higher E/V.

An important consequence of spacial gradients is that probably no more than one-half of the target could turn into a plasma. Therefore, signatures from the plasma will most likely be contaminated by "ordinary" hadronic processes occurring in the cooler half. Unfolding the contributions from various depths in the target will be necessary. In any case, the naive homogeneous plasma-ball idealization of nuclear collisions will not be adequate.

We now come to the question of whether the energy density achieved is in fact high enough to produce a plasma. For an ideal Stefan-Boltzmann gas of Ng gluons, N_c colors, N_f flavors, the energy density is

$$(E/V)_{SB} = \frac{\pi^2}{15} \left(N_g + \frac{7}{4}\, N_c\, N_f\right) T^4 \equiv K_{SB}\, T^4 \quad . \tag{27}$$

For SU(3) up-down-glue matter, $(E/V)_{SB}$ is plotted in Fig. (2) versus temperature. In comparison, Monte Carlo data[4,5] for SU(2)

and SU(3) are also shown. It is important to emphasize that these data apply strictly to pure glue matter ($N_f = 0$). We have simply rescaled those data in Fig. (2) with K_{SB} appropriate to ($N_g = 8$, $N_c = 3$, $N_f = 2$). This rescaling cannot be expected to be accurate but only gives a qualitative indication of where deviations from the SB limit may occur. We see that only for temperatures $\gtrsim$ 300 MeV is the plasma describable as a perturbative gas. For $T < 250$ MeV, large deviations from the SB limit occur. Also note the qualitative change of E/V at $T_c \approx 220$ MeV, which could be considered as the phase transition point.

The maximum energy density reached in U + U collisions at a depth 14 fm is also shown in Fig. 2. The conservative TCM seems to fall short of the transition point, while SDM seems to probe the transition temperature region directly. Note the remarkably limited range of energy densities accessible in both models for the ISR energy range $\sqrt{s} = 30$–100 GeV per nucleon. Thus, at best only the vicinity of the phase transition point is probed in the fragmentation regions. This, of course, is exciting enough! Nevertheless, it is important to emphasize that near T_c non-perturbative effects are important as seen by the large deviation of the Monte Carlo data from the SB limit. Therefore, signatures from the plasma probably cannot be calculated by perturbative methods. The truly perturbative domain requires at least 10 GeV/fm^3 as seen in Fig. (2).

In conclusion, we have constructed simple analytical models for estimating the spacial dependence of the energy deposition in nuclear collisions. Only the fragmentation regions were considered. The conservative Trailing Cascade scenario leads to almost homogeneous energy deposition, which is, however, too small to be of real interest. The optimistic Sequential Decay scenario along the lines of McLerran et al.[2] yields significantly higher energy densities, but at the price of greater spacial gradients. The difference of TCM and SDM already points to the sensitivity of nuclear collisions to the space-time structure of hadronic processes. Even if no plasma is produced, the fragmentation regions promise to provide insight into those processes. An important

future problem will be to analyze available hadron-nucleus data to see which of the models is closer to reality.

Acknowledgments:

Stimulating discussions with P. Danielewicz, A. Klar, L. McLerran, H. Satz, and J. Kuti are gratefully acknowledged. This work was supported by the Director, Office of Energy Research, Division of Nuclear Physics of the Office of High Energy and Nuclear Physics of the U.S. Department of Energy under Contract DE-AC03-76SF00098.

References

1. See reviews in "1st Workshop on Ultra-Relativistic Nuclear Collisions," LBL-8957, UC-34c, CONF-7905107, May 1979.
2. R. Anishetty, P. Koehler, L. McLerran, Phys. Rev. 22D, 2793 (1980).
3. D.J. Gross, R.D. Pisarski, L.G. Yaffe, Rev. Mod. Phys. 53, 43 (1981).
4. J. Engels, F. Karsch, I. Montvay, H. Satz, Phys. Lett. 101B, 89 (1981), 102B, 332 (1981).
5. I. Montvay, E. Pietarinnen, Phys. Lett. 110B, 148 (1982).

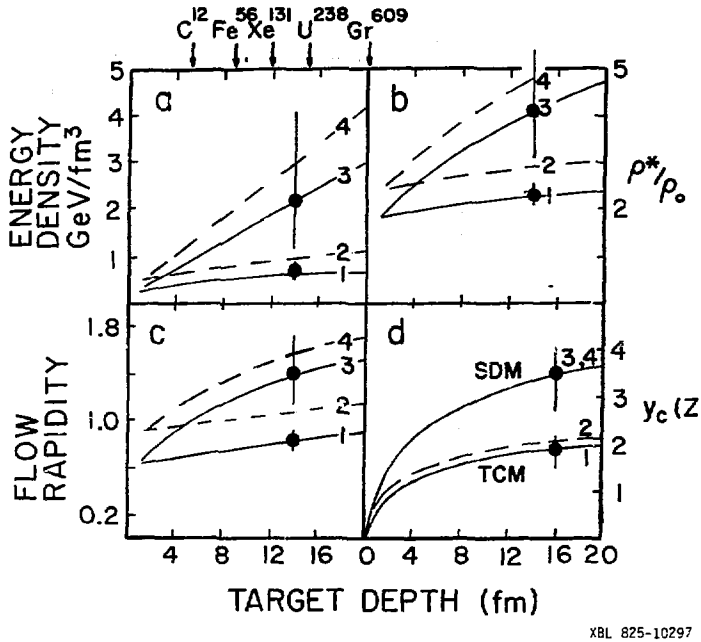

Fig. 1. Solid curves 1,3 refer to TCM,SDM at $\sqrt{s}$ = 30 GeV. Dashed curves 2,4 refer to TCM,SDM at $\sqrt{s}$ = 100 GeV. The maximum comoving frame energy density (a) and compression (b) are shown vs the depth into the target. The flow rapidity $y_f(z)$ and the stopping rapidity $y_c(z)$ are shown in (c) and (d). The error bar denotes the variation in the predictions when the scale parameter τ_0 varies between 0.5 to 2.0 fm/c (for the curves τ_0 = 1 fm/c).

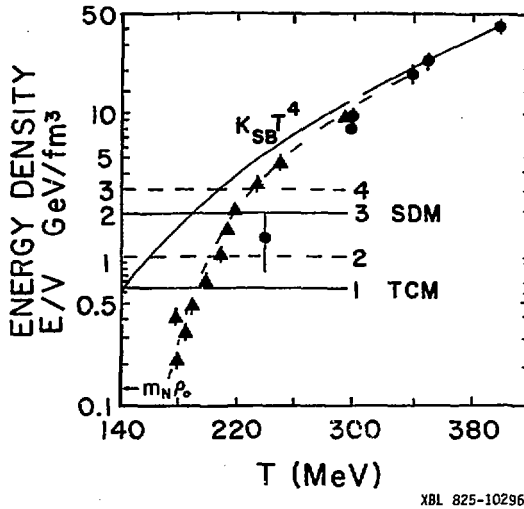

Fig. 2. Energy density versus temperature for ideal Stefan-Boltzmann plasma ($K_{SB} = 12.2$). The Monte Carlo data for lattice SU(2) (triangles[4]) and SU(3) (dots[5]) are shown rescaled to ($N_g = 8$, $N_f = 2$) matter. The maximum energy densities in U + U collisions at a depth 14 fm are indicated for $\sqrt{s}$ = 30-100 GeV/nucleon from Fig. 1.